

Article

Series of Broad Resonances in Atomic Three-Body Systems

Daniel Diaz, Zoltan Papp * and Chi-Yu Hu

Department of Physics and Astronomy, California State University Long Beach, Long Beach, CA, USA; ddiaz006@ucr.edu (D.D.); Chiyu.Hu@csulb.edu (C.Y.H.)

* Correspondence: Zoltan.Papp@csulb.edu

Academic Editor: James F. Babb

Received: 27 January 2016; Accepted: 14 June 2016; Published: 20 June 2016

Abstract: We re-examine the series of resonances found earlier in atomic three-body systems by solving the Faddeev-Merkuriev integral equations. These resonances are rather broad and line up at each threshold with gradually increasing gaps. This lining up takes place in the same way for all thresholds and is irrespective of the spatial symmetry. We relate these resonances to the Gailitis mechanism, which is a consequence of the polarization potential.

Keywords: resonances; three-body Coulomb systems; Faddeev-Merkuriev equations

1. Introduction

A couple of years ago we observed an accumulation of resonances above the thresholds [1,2]. Other independent calculations have not confirmed these findings, only a few narrow resonances have been independently calculated. This is understandable, since calculation of broad resonances, especially in a multi-body system, is very complicated. The wave function of narrow resonances behaves very much like a bound-state wave function, so they can be calculated by some slight modification of bound state techniques. The most common method is the complex rotation of coordinates. This technique renders the resonance state wave function to a square integrable one, and thus standard techniques like variational expansion of the wave function become applicable. These methods, however, run into technical difficulties for broad resonances. Here, to uncover the resonances, they need a large rotation angle and the rotated continuum becomes more and more scattered making the identification of resonances increasingly difficult.

Our method is different. We start with the Faddeev integral equations with the modification proposed by Merkuriev [3] and solve them by using the Coulomb-Sturmian potential separable expansion method [4,5]. Since the investigations of References [1,2] we improved the technique in Reference [6] making it more amenable to calculate broad resonances. Therefore, in Section 2 we outline our technique of solving the Faddeev-Merkuriev integral equations for resonant states while in Section 3 we show our results for $e - Ps$ resonances. Finally, we summarize our findings and provide an explanation for the formation of the series of broad resonances.

2. Calculation of Coulomb Three-Body Resonances

2.1. Faddeev-Merkuriev Integral Equations

The Hamiltonian of an atomic three-body system is given by

$$H = H^0 + v_1^C + v_2^C + v_3^C \quad (1)$$

where H^0 is the three-body kinetic energy operator and v_α^C denotes the Coulomb interaction of each subsystem $\alpha = 1, 2, 3$. We use the usual configuration-space Jacobi coordinates x_α and y_α , where x_α is

the distance between the pair (β, γ) and y_α is the distance between the center of mass of the pair (β, γ) and the particle α . The potential v_α^C , the interaction of the pair (β, γ) , appears as $v_\alpha^C(x_\alpha)$. In an atomic three-body system, two particles always have the same sign of charge. Without loss of generality, we can assume that they are particles 1 and 2, and thus v_3^C is a repulsive Coulomb potential.

The wave function of a three-particle system is very complicated. It exhibits different asymptotic behaviors reflecting the possible asymptotic fragmentations. In the Faddeev approach we split the wave function into components such that each component describes only one kind of asymptotic fragmentation [3]. The components satisfy a set of coupled equations, the Faddeev equations.

The Hamiltonian (1) is defined in the three-body Hilbert space. Therefore, the two-body potential operators are formally embedded in the three-body Hilbert space,

$$v_\alpha^C = v_\alpha^C(x_\alpha)\mathbf{1}_{y_\alpha} \tag{2}$$

where $\mathbf{1}_{y_\alpha}$ is a unit operator in the two-body Hilbert space associated with the y_α coordinate.

The Coulomb potential is a long range potential as it modifies the motion even at asymptotic distances. On the other hand, it also possesses some features of a short-range potential as it correlates the particles strongly and supports two-body bound states. These two properties are contradictory and require different treatments. In Merkuriev’s approach the three-body configuration space is divided into different asymptotic regions [7]. The two-body asymptotic region Ω_α is defined as a part of the three-body configuration space where the conditions

$$(|x_\alpha|/x_0)^\nu < |y_\alpha|/y_0 \tag{3}$$

with parameters $x_0 > 0$, $y_0 > 0$ and $\nu > 2$ are satisfied. It has been shown that in Ω_α the short-range character of the Coulomb potential prevails, while in the complementary region the long-range character of the Coulomb potential becomes dominant.

Therefore, we split the Coulomb potential in the three-body configuration space into short-range and long-range parts

$$v_\alpha^C = v_\alpha^{(s)} + v_\alpha^{(l)} \tag{4}$$

The splitting is carried out with the help of a splitting function ζ_α ,

$$v_\alpha^{(s)}(x_\alpha, y_\alpha) = v_\alpha^C(x_\alpha)\zeta_\alpha(x_\alpha, y_\alpha) \tag{5}$$

$$v_\alpha^{(l)}(x_\alpha, y_\alpha) = v_\alpha^C(x_\alpha) [1 - \zeta_\alpha(x_\alpha, y_\alpha)] \tag{6}$$

The function ζ_α vanishes asymptotically within the three-body sector, where $x_\alpha \sim y_\alpha \rightarrow \infty$, and approaches 1 in the two-body asymptotic region Ω_α , where $x_\alpha \ll y_\alpha \rightarrow \infty$. As a result, in the three-body sector, the short-range potential $v_\alpha^{(s)}$ vanishes and long-range potential $v_\alpha^{(l)}$ approaches v_α^C . In practice, the functional form

$$\zeta_\alpha(x_\alpha, y_\alpha) = 2 / \{1 + \exp [(x_\alpha/x_0)^\nu / (1 + y_\alpha/y_0)]\} \tag{7}$$

is used. Typical shapes for $v^{(s)}$ and $v^{(l)}$ are shown in Figures 1 and 2. In fact, these parameters were adopted in our $e - Ps$ calculations. We can see that $v^{(l)}$ is a valley which opens up as y_α goes to infinity and becoming shallower and shallower. Finally, in the $y_\alpha \rightarrow \infty$ limit there is no two-body bound state in x_α .

The Coulomb potential v_3^C is repulsive. So, it does not support bound states and there are no two-body channels associated with this fragmentation. Consequently, the entire v_3^C can be considered as a long-range potential. Then the long-range Hamiltonian is defined as

$$H^{(l)} = H^0 + v_1^{(l)} + v_2^{(l)} + v_3^C \tag{8}$$

and the three-body Hamiltonian looks like an ordinary three-body Hamiltonian with only two short range interactions

$$H = H^{(l)} + v_1^{(s)} + v_2^{(s)} \tag{9}$$

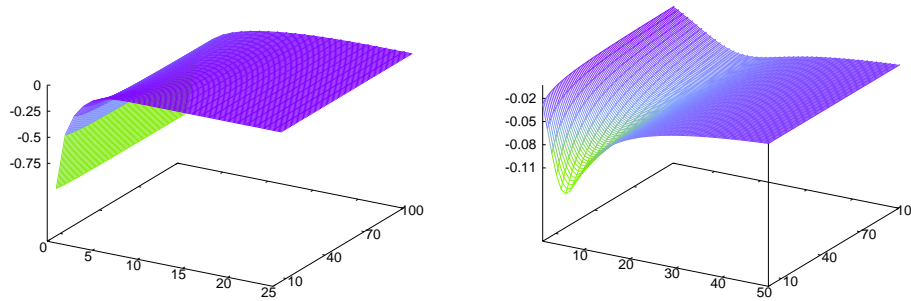


Figure 1. Short range ($v^{(s)}$) and long range ($v^{(l)}$) parts of an attractive Coulomb potential. The parameters are $Z = -1$, $x_0 = 4$, $y_0 = 12$ and $\nu = 2.1$.

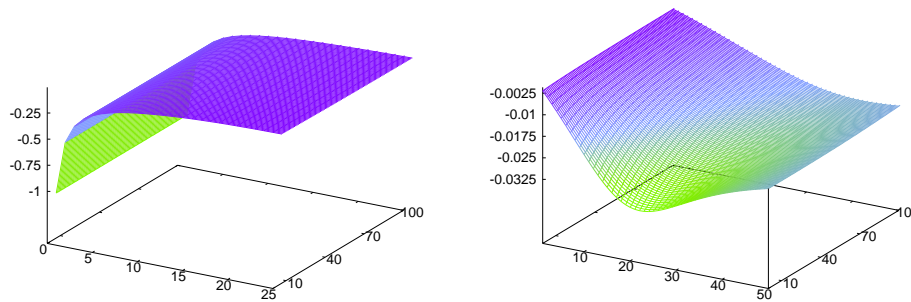


Figure 2. Short range ($v^{(s)}$) and long range ($v^{(l)}$) parts of an attractive Coulomb potential. The parameters are $Z = -1$, $x_0 = 15$, $y_0 = 35$ and $\nu = 2.1$.

So, we split the wave function into two components only

$$|\Psi\rangle = |\psi_1\rangle + |\psi_2\rangle. \tag{10}$$

Then for components, we have the set of Faddeev equations,

$$\begin{aligned} (E - H_1^{(l)})|\psi_1\rangle &= v_1^{(s)}|\psi_2\rangle \\ (E - H_2^{(l)})|\psi_2\rangle &= v_2^{(s)}|\psi_1\rangle \end{aligned} \tag{11}$$

where

$$H_\alpha^{(l)} = H^{(l)} + v_\alpha^{(s)} \tag{12}$$

By adding these two equations we recover the original Schrödinger equation. So, the Faddeev procedure is a clever way of solving the quantum mechanical Schrödinger equation. We can write these differential equations into an integral equation form

$$\begin{aligned} |\psi_1\rangle &= G_1^{(l)}(E)v_1^{(s)}|\psi_2\rangle \\ |\psi_2\rangle &= G_2^{(l)}(E)v_2^{(s)}|\psi_1\rangle \end{aligned} \tag{13}$$

where $G_\alpha^{(l)}(E) = (E - H_\alpha^{(l)})^{-1}$. With Merkuriev’s procedure Faddeev’s aim is achieved for the Coulomb potential as well. Now each component describes only one kind of asymptotic fragmentation.

If particles 1 and 2 are identical particles, the Faddeev components $|\psi_1\rangle$ and $|\psi_2\rangle$, in their own natural Jacobi coordinates, must have the same functional forms

$$\langle x_1 y_1 | \psi_1 \rangle = \langle x_2 y_2 | \psi_2 \rangle \tag{14}$$

On the other hand, by interchanging particles 1 and 2, we have

$$\mathcal{P}_{12} |\psi_1\rangle = p |\psi_2\rangle \tag{15}$$

where $p = \pm 1$, depending the total spin of the two identical particles. So, ψ_1 and ψ_2 are not independent, and to determine one of them we need only one equation

$$|\psi_1\rangle = G_1^{(l)} v_1^{(s)} p \mathcal{P}_{12} |\psi_1\rangle \tag{16}$$

As we can see, we can easily incorporate the identity of particles into the Faddeev formalism, and this even leads to a considerable simplification of the equations.

2.2. Solution Method

In order that we can solve the Faddeev-Merkuriev integral equations we represent them in Coulomb–Sturmian (CS) basis. The CS functions are given by

$$\langle r | nl; b \rangle = \sqrt{\frac{n!}{(n + 2l + 1)!}} \exp(-br) (2br)^{l+1} L_n^{(2l+1)}(2br) \tag{17}$$

where L denotes the Laguerre polynomials, l is angular momentum, n is the radial quantum number and b is a parameter. With $\langle r | \widetilde{nl}; b \rangle \equiv \langle r | nl; b \rangle / r$, the orthogonality and completeness relations take the forms

$$\langle \widetilde{n'l}; b | nl; b \rangle = \langle n'l; b | \widetilde{nl}; b \rangle = \delta_{nn'} \tag{18}$$

and

$$\mathbf{1} = \lim_{N \rightarrow \infty} \sum_{n=0}^N |\widetilde{nl}; b\rangle \langle nl; b| = \lim_{N \rightarrow \infty} \sum_{n=0}^N |nl; b\rangle \langle \widetilde{nl}; b| \tag{19}$$

The three-body Hilbert space is a direct product of two-body Hilbert spaces, so, as a basis, we may take the angular-momentum-coupled direct product of the two-body bases,

$$|n\nu l \lambda; b\rangle_\alpha = |nl; b\rangle_\alpha \otimes | \nu \lambda; b\rangle_\alpha, \quad (n, \nu = 0, 1, 2, \dots) \tag{20}$$

where $|nl; b\rangle_\alpha$ and $| \nu \lambda; b\rangle_\alpha$ are associated with the coordinates x_α and y_α , respectively. With this basis, the completeness relation takes the form (with angular momentum summation implicitly included)

$$\mathbf{1} = \lim_{N \rightarrow \infty} \sum_{n, \nu=0}^N |n\nu l \lambda; b\rangle_\alpha \langle n\nu l \lambda; b| = \lim_{N \rightarrow \infty} \mathbf{1}_\alpha^N \tag{21}$$

We insert a unit operator into the Faddeev Equations (13)

$$\begin{aligned} |\psi_1\rangle &= \lim_{N \rightarrow \infty} G_1^{(l)}(E) \mathbf{1}_1^N v_1^{(s)} \mathbf{1}_2^N |\psi_2\rangle \\ |\psi_2\rangle &= \lim_{N \rightarrow \infty} G_2^{(l)}(E) \mathbf{1}_2^N v_2^{(s)} \mathbf{1}_1^N |\psi_1\rangle \end{aligned} \tag{22}$$

and keep N finite. This amounts to approximating $v_\alpha^{(s)}$ in the three-body Hilbert space by a separable form

$$\begin{aligned}
 v_\alpha^{(s)} &= \lim_{N \rightarrow \infty} \mathbf{1}_\alpha^N v_\alpha^{(s)} \mathbf{1}_\beta^N \approx \mathbf{1}_\alpha^N v_\alpha^{(s)} \mathbf{1}_\beta^N \\
 &\approx \sum_{n,\nu,n',\nu'=0}^N |n\nu l \widetilde{\lambda}, b\rangle_\alpha v_{\alpha\beta}^{(s)} |n'\nu' l' \widetilde{\lambda}', b\rangle_\beta
 \end{aligned}
 \tag{23}$$

where $v_{\alpha\beta}^{(s)} = {}_\alpha \langle n\nu l \lambda; b | v_\alpha^{(s)} | n'\nu' l' \lambda'; b \rangle_\beta$. In general, we can calculate these matrix elements numerically. The completeness of the CS basis guarantees the convergence of the expansion with increasing N and angular momentum channels.

This approximation turns the homogeneous Faddeev-Merkuriev equation into a matrix equation for the component vector

$$\begin{aligned}
 \psi_1 &= \underline{G}_1^{(l)}(E) v_{12}^{(s)} \psi_2 \\
 \psi_2 &= \underline{G}_2^{(l)}(E) v_{21}^{(s)} \psi_1
 \end{aligned}
 \tag{24}$$

where

$$\underline{G}_\alpha^{(l)} = {}_\alpha \langle n\nu l \widetilde{\lambda}; b | G_\alpha^{(l)} | n'\nu' l' \widetilde{\lambda}'; b \rangle_\alpha
 \tag{25}$$

The Green’s operator $\underline{G}_\alpha^{(l)}$ is too complicated for a direct evaluation. However, in the Faddeev-Merkuriev equation it generates only α -type asymptotic configurations where particles β and γ form bound or scattering states. Therefore, in this region of the three-body configuration space $G_\alpha^{(l)}$ can be linked to a simpler Green’s operator

$$G_\alpha^{(l)}(z) = \tilde{G}_\alpha(z) + \tilde{G}_\alpha(z) U_\alpha G_\alpha^{(l)}(z)
 \tag{26}$$

where $\tilde{G}_\alpha(z) = (z - \tilde{H}_\alpha)^{-1}$ and $U_\alpha = H_\alpha^{(l)} - \tilde{H}_\alpha$ with

$$\tilde{H}_\alpha = H^0 + v_\alpha^C + u_\alpha^{(l)}
 \tag{27}$$

Here $u_\alpha^{(l)}(y_\alpha) = Z_\alpha(Z_\beta + Z_\gamma)e^2/y_\alpha$. This way U_α is of short range type, and can be approximated on the CS basis as before.

In our Jacobi coordinates, the three-particle kinetic energy can be written as a sum of two-particle free Hamiltonians

$$H^0 = h_{x_\alpha}^0 + h_{y_\alpha}^0
 \tag{28}$$

Thus the Hamiltonian \tilde{H}_α of Equation (27) appears as a sum of two two-body Hamiltonians acting on different coordinates

$$\tilde{H}_\alpha = h_{x_\alpha} + h_{y_\alpha}
 \tag{29}$$

where $h_{x_\alpha} = h_{x_\alpha}^0 + v_\alpha^C(x_\alpha)$ and $h_{y_\alpha} = h_{y_\alpha}^0 + u_\alpha^{(l)}(y_\alpha)$. So, \tilde{G}_α is a resolvent of the sum of two commuting Hamiltonians h_{x_α} and h_{y_α} . Such resolvents can be expressed as a convolution integral of two-body Green’s operators

$$\begin{aligned}
 \tilde{G}_\alpha(z) &= (z - h_{y_\alpha} - h_{x_\alpha})^{-1} \\
 &= \frac{1}{2\pi i} \oint_{\mathcal{C}} dz' (z - h_{y_\alpha} - z')^{-1} (z' - h_{x_\alpha})^{-1} \\
 &= \frac{1}{2\pi i} \oint_{\mathcal{C}} dz' g_{y_\alpha}(z - z') g_{x_\alpha}(z')
 \end{aligned}
 \tag{30}$$

where $g_{x_\alpha}(z) = (z - h_{x_\alpha})^{-1}$ and $g_{y_\alpha}(z) = (z - h_{y_\alpha})^{-1}$. The contour \mathcal{C} should be taken in a counterclockwise direction around the singularities of g_{x_α} such that g_{y_α} is analytic on the domain

encircled by \mathcal{C} . So, to calculate the matrix elements $\tilde{\mathcal{G}}_\alpha$, we need to calculate a contour integral of the two-body Green's matrices \underline{g}_{y_α} and \underline{g}_{x_α} . Those two-body Coulomb Green's matrix elements can be calculated analytically for complex energies by continued fractions [8]. This is an exact representation of \underline{g}_{x_α} and \underline{g}_{y_α} , consequently the thresholds are at the exact locations with the proper Coulomb degeneracy.

In this work, we calculate the negative energy resonances of the $e - Ps$ three-body system. We need to solve (16) such that in x_1 we have the $e^- - e^+$ pair. So, g_{x_1} is a Coulomb Green's operator with a branch-cut on the $[0, \infty)$ interval and accumulation of infinitely many bound states at zero energy. On the other hand $u_1^{(l)}(y_1)$ is absent and g_{y_1} is a free Green's operator with branch-cut singularity on the $[0, \infty)$ interval. The resonances are at $E = E_r - i\Gamma/2$. First, we need to formulate $\tilde{G}_1(E) = \tilde{G}_1(E_r + i\varepsilon)$, with $\varepsilon > 0$, then we need continue analytically to $E = E_r - i\Gamma/2$. For this purpose we take the contour of Figure 3. With $\varepsilon > 0$ the singularities of g_{x_1} and g_{y_1} are well separated and the contour encircles the spectrum of g_{x_1} without touching the singularities of g_{y_1} . Then we change the contour analytically as shown in Figure 4. The contour encircles some low-lying singularities of g_{x_1} resulting in its residue, while the other part of the contour is deformed to an integration along a straight line parallel to the imaginary axis. Now, we can take the $\varepsilon \rightarrow -\Gamma/2$ transition. By doing so, the poles of g_{x_1} submerge into the second Riemann sheet of g_{y_1} but the contour stays away from the singularities of g_{y_1} (Figure 5).

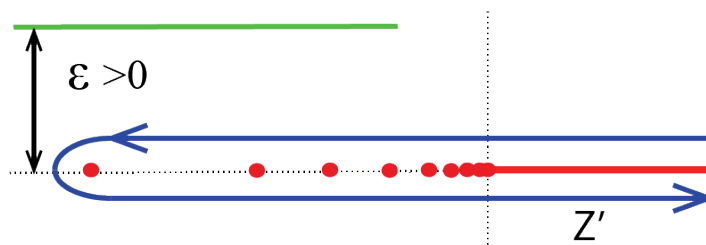


Figure 3. The analytic structure of $g_{y_1}(E_r + i\varepsilon - z')g_{x_1}(z')$ as a function of z' with $\varepsilon > 0$. The operator $g_{x_1}(z')$ has a branch-cut on the $[0, \infty)$ interval and accumulation of infinitely many bound states at zero energy, while $g_{y_1}(E + i\varepsilon - z')$ has a branch-cut on the $(-\infty, E + i\varepsilon]$ interval. The contour \mathcal{C} encircles the spectrum of g_{x_1} and avoids the singularities of g_{y_1} .

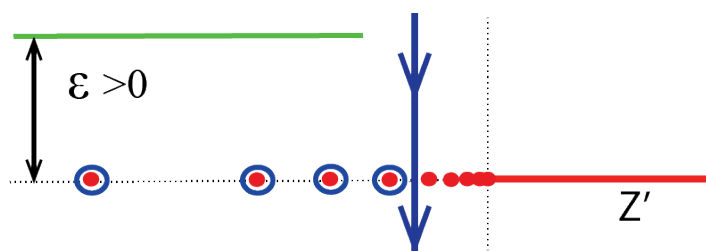


Figure 4. The contour of Figure 3 is deformed analytically such that it encircles the low-lying bound-state poles of g_{x_1} and the other part is taken along an imaginary direction.

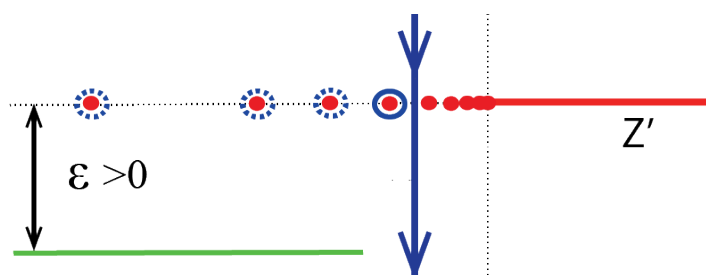


Figure 5. Analytic continuation to $\varepsilon = -\Gamma/2$. The low-lying poles of g_{x_1} submerge onto the second Riemann sheet of g_{y_1} , and they are denoted by dotted contour.

In calculating the three-body Coulomb Green’s matrix \tilde{G}_x the mathematical condition for the integral in Equation (30) is that the contour \mathcal{C} should encircle the spectrum of one of the two-body Green’s operators without incorporating the spectrum of the other. In References [1,2] the contour was taken such a way that it encircled the singularities of g_y . However, for resonant-state energies, the bound-state poles of g_x penetrate into the continuous spectrum of g_y . Then to meet the requirement for the contour \mathcal{C} , the path around the spectrum of g_y had to be taken in such a way that it descends down into the unphysical Riemann sheet. However, the integration on the unphysical sheet is rough, the Green’s matrix exhibits violent changes, and this is getting even worse for broader resonances as the contour dives deeper into the second sheet. A singularity is always very prominent, so this numerical inaccuracy does not eliminate the resonance poles and does not mask the whole phenomenon, but it makes the identification of individual resonances, especially the broad ones, less trustworthy. The contour adopted here avoids this pitfall. No integration goes on the unphysical sheet, the path of integration is far away from any singularities, so we get very reliable results with just a few integration points.

3. Results

We calculate the $L = 0$ resonances of the $e - Ps$ system. We used atomic units throughout. We have to select l and λ such that $l - \lambda = 0$. The two electrons are identical and the two spins can be coupled either to $S = 0$ or $S = 1$. The $S = 0$ state is antisymmetric with respect to the exchange of the spin coordinates, and consequently it should be symmetric with respect to exchange the electron spatial coordinates. So, if $S = 0$ we have $p = 1$ in Equation (16), while if $S = 1$ we have $p = -1$.

We have two parameters to vary in the calculations. One is the scale parameter b . We found a good stability in our results with $b = 0.25$. The other parameter is N , the maximal radial quantum number in the expansion of the potentials in each angular momentum channel and in x and y coordinates. We can see that while the narrow resonances are very stable with increasing N , the broad resonances are not so. This is understandable since the broad resonances are always hard to calculate. However, this inaccuracy does not change the whole picture. Individual resonances may vary a little bit with increasing N and with changing the parameters x_0 and y_0 , but the series of resonances originating from the threshold are there. We found $N = 32$ big enough for stable results.

Figures 6 and 7 show the resonances between various thresholds using three cut-off parameters. False resonances may occur in the Faddeev-Merkuriev method. They are associated with the possible bound states of $H^{(l)}$. However, by taking x_0 about the same size as the two-body subsystem in x , and varying (x_0, y_0) , we can avoid them. We can see that the broad resonances line up along a straight line with increasing spacings. It seems that at higher thresholds we have more lines.

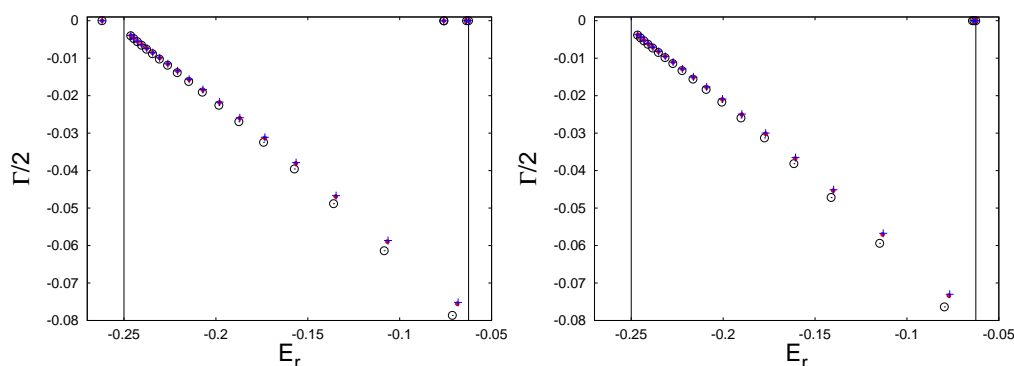


Figure 6. 1S and 3S resonances of the $e - Ps$ system between the $n = 1$ and $n = 2$ thresholds. Black circles indicate data using cut-off parameters $x_0 = 4, y_0 = 12$, red dots indicate data using cut-off parameters $x_0 = 8, y_0 = 24$, and blue + symbols indicate data using cut-off parameters $x_0 = 8, y_0 = 12$. Thresholds indicated with vertical bars.

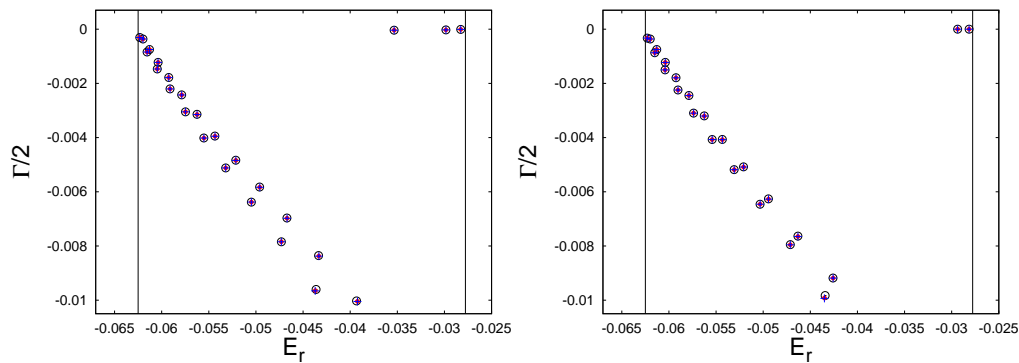


Figure 7. 1S and 3S resonances of the $e - Ps$ system between the $n = 2$ and $n = 3$ thresholds. Black circles indicate data using cut-off parameters $x_0 = 12, y_0 = 30$, red dots indicate data using cut-off parameters $x_0 = 15, y_0 = 35$, and blue + symbols indicate data using cut-off parameters $x_0 = 15, y_0 = 30$. Thresholds indicated with vertical bars.

4. Summary and Interpretation

In this work, we re-examined the broad resonances lining up around thresholds. We solved the Faddeev-Merkuriev integral equations by adopting a Coulomb-Sturmian based separable expansion approach on the potential in the three-body configuration space. This method approximates only the asymptotically irrelevant short range potentials. The asymptotically relevant parts are kept in the Green's operator \tilde{G}_α , and its CS matrix elements have been evaluated as a complex convolution integral of the two-body Green's matrices. The adopted contour makes the calculation of \tilde{G}_α numerically exact, even for very broad resonances, and ensures that all the thresholds are at the right location. The only real approximation is that the basis in each of the coordinates is truncated to a finite N , but we found $N = 32$ to be big enough for very reliable results.

We found that some of those resonances lie along a straight line. From Figure 6 we can see that for those resonances the ratio $\epsilon_m/\Delta\epsilon_m \approx 1.23 \pm 0.03$, where ϵ is the center of mass energy measured from the thresholds. They must have a common origin.

It appears that these series of resonances have not been reproduced by other methods. Careful examination and comparison with previous resonance calculations revealed that long-lived resonances were calculated previously along with Feshbach resonances. They are called shape resonances in the atomic physics community. As early as 1962-1963 in the work of Gailitis and Damburg [9] their presence as T-matrix oscillations above thresholds were calculated.

Hu and Caballero [10] carried out a six open-channel high precision calculation of the $e^+ + H$ ($n = 2$) scattering system using the Faddeev-Merkuriev differential equations. The calculation involves no intermediate approximations nor truncation of any kind. The numerical method solved a half million coupled linear equations. All scattering properties were calculated in the range of energy just above the Ps ($n = 2$) formation threshold. The results display singularities of the K -matrix ($\tan \delta$) (the phase shift jumps by π), the cross section maxima and the six channel wave amplitudes. All display three resonances within a cutoff distance of $1000a_0$, where a_0 is the Bohr radius, in channels $p + Ps$ ($n = 2, l = 0$) and $p + Ps$ ($n = 2, l = 1$). These calculations revealed a previously unknown, but relatively simple formation mechanism for these kind of resonances.

For the Ps ($n = 2$) target, the Coulomb degeneracy allows the incoming proton to induce a first order constant electric dipole moment μ_1 on the target, known as the first order Stark effect. By analyzing the channel wave functions in resonance channels $p + Ps$ ($n = 2, l = 0$) and $p + Ps$ ($n = 2, l = 1$) Hu and Caballero [10] found that the resonant conditions arise when the center-of-mass energy of the proton satisfy the simple relations

$$\epsilon_m = m\mu_1/y_m^2, \quad \epsilon_m/\Delta\epsilon_m = \text{constant} \quad (31)$$

where $m = 1, 2, \dots$ integer, and y_m is the location (Jacobi coordinate) of the proton at the resonance.

The Stark effect is a universal phenomenon. Furthermore, if the target is not degenerate the second order Stark effect takes place. The induced electric dipole moment is $\mu_1 = \alpha/y^2$, where α is the second order polarizability. Then the resonant condition becomes

$$\epsilon_m = m\mu_1/y_m^2 = m\alpha/y_m^4, \quad m = 1, 2, \dots \quad (32)$$

These explain our observations that the resonances are lining up from the thresholds with increasing spacing. Also, in the energy region between $n = 2$ and $n = 3$ thresholds the induced electric dipole moment μ is different for $l = 0$ and $l = 1$, so we observe some splitting of the lines as well.

Author Contributions: This method of calculating three-body resonances has been designed by Zoltan Papp, the calculations were carried out by Daniel Diaz, and the interpretation has been provided by Chi-Yu Hu.

Author Contributions: The author declare no conflict of interest.

References

1. Papp, Z.; Darai, J.; Mezei, J.Z.; Hlousek, Z.T.; Hu, C.-Y. Accumulation of three-body resonances above two-body thresholds. *Phys. Rev. Lett.* **2005**, *94*, 143201.
2. Mezei, J.Z.; Papp, Z. Efimov resonances in atomic three-body systems. *Phys. Rev. A* **2006**, *73*, 030701(R).
3. Faddeev, L.D.; Merkuriev, S.P. *Quantum Scattering Theory for Several Particle Systems*; Kluwer: Dordrecht, The Netherlands, 1993.
4. Papp, Z. Three-potential formalism for the three-body Coulomb scattering problem. *Phys. Rev. C* **1997**, *55*, 1080–1087.
5. Papp, Z.; Hu, C.-Y.; Hlousek, Z. T.; Konya, B.; Yakovlev, S.L. Three-potential formalism for the three-body scattering problem with attractive Coulomb interactions. *Phys. Rev. A* **2001**, *63*, 062721.
6. Keller, S.; Marotta, A.; Papp, Z. Faddeev-Merkuriev integral equations for atomic three-body resonances. *J. Phys. B* **2009**, *42*, 044003.
7. Merkuriev, S.P. On the three-body Coulomb scattering problem. *Ann. Phys.* **1980**, *130*, 395–426.
8. Demir, F.; Hlousek, A.T.; Papp, Z. Coulomb-Sturmian matrix elements of the Coulomb Green's operator. *Phys. Rev. A* **2006**, *74*, 014701.
9. Gailitis, M.; Damburg, R. Some features of the threshold behavior of the cross sections for excitation of hydrogen by electrons due to the existence of a linear Stark effect in hydrogen. *J. Exp. Theor. Phys.* **1963**, *44*, 1644–1649.
10. Hu, C.-Y.; Caballero, D. Long-range correlation in positron-hydrogen scattering near the threshold of Ps ($n = 2$) formation. *J. Mod. Phys.* **2013**, *4*, 622–627.



© 2016 by the authors; licensee MDPI, Basel, Switzerland. This article is an open access article distributed under the terms and conditions of the Creative Commons Attribution (CC-BY) license (<http://creativecommons.org/licenses/by/4.0/>).